Robust Finite-Time Control of a Multirotor System via an Improved Optimized Homogeneous Twisting Control: Design and Validation

Aimen Abdelhak Messaoui[1], Omar Mechali[1], Ali Zakaria Messaoui[2] and Iheb Eddinde Smaali[1]
[1]*Ecole Supérieure Ali Chabati, Réghaia, Algeria*
[2]*Laboratoire de Commande des Systèmes Complexes et Simulateurs, Ecole Militaire Polytechnique, Bordj El-Bahri, Algeria*

Keywords: The Attitude Tracking Control, Finite-Time Stability, Homogeneous Sliding Mode Control, Pixhawk Autopilot, Quadrotor Aircraft.

Abstract: This paper presents theoretical and practical aspects of finite-time tracking control of a multirotor attitude system. The vehicle is subjected to matched lumped disturbances. Inspired by the homogeneity theory, an Improved Optimized Homogeneous Twisting Control (IOHTC) is proposed to deal with the fast dynamics' response of the attitude states. Within the designed control scheme, the chattering issue of discontinuous Sliding Mode Control (SMC) techniques can be mitigated due to the continuous control signal that is generated by a non-switching function in the form of $|x|^{\alpha}\mathrm{sign}(x), x \in R, \alpha \in R+$. Besides, finite-time convergence of the system's states can be ensured to achieve accurate control. It is worth mentioning that the disturbance rejection does not require the design of an observer since the control law integrates a compensation term. Stability analysis of the closed-loop system is rigorously investigated by using a homogeneous Lyapunov function. From the practical aspect, the control algorithm is embedded onboard the quadrotor's autopilot through a model-based design approach. A comparative study is made involving the proposed IOHTC strategy and three other controllers. The obtained results show that the suggested controller yields performance improvement regarding accuracy and robustness. Meanwhile, the chattering effect of conventional SMC is remarkably alleviated.

1 INTRODUCTION

The quadrotor is among the most often used multirotor aircraft because of its particular flight mode, variety of sizes, and exceptional hovering capabilities. Unfortunately, it is also considered a well-known underactuated mechanical system. However, since its invention in 1907, quadcopters have found use in a wide range of application fields (O. Mechali J. I., 2021) (O. Mechali J. I., 2021). However, despite its alluring qualities, this kind of system faces real challenges, especially in terms of control. Accurate and robust aircraft attitude control is necessary for autonomous quadrotor flying. Since a quadrotor is a nonlinear system with highly coupled dynamics, it is susceptible to internal modeling errors, parametric uncertainty, and external disturbances. Consequently, developing the system attitude controller becomes challenging. In order to perform the objectives of the flying mission, this aircraft's autonomous flight requires a sophisticated control scheme. Additionally, the controller design appears based on robustness, high control accuracy, and quick convergence.

SMC, among other robust control approaches, is an active topic in the unmanned aerial vehicle community nowadays for controlling quadrotor aircraft (S. Benmansour, 2023) (S. G. Khan, 2019). The simplicity of design and the fast response are among the benefits of such methods. In addition, it accurately compensates for matched disturbances. Several recent research works have focused on synthesizing and implementing robust SMC-based control laws for disturbance handling in the quadrotor system. For example, through an integral SMC-based approach, the study described in (S. Ullah, 2020) seeks to enhance the stability of an underactuated quadcopter. A robust backstepping-SMC control law is suggested in a further inspired study (Almakhles, 2020) to deal with the quadrotor model with disturbances. However, because a linear switching manifold has been employed, it is guaranteed that the

Messaoui, A., Mechali, O., Messaoui, A. and Smaali, I.
Robust Finite-Time Control of a Multirotor System via an Improved Optimized Homogeneous Twisting Control: Design and Validation.
DOI: 10.5220/0012086700003546
In *Proceedings of the 13th International Conference on Simulation and Modeling Methodologies, Technologies and Applications (SIMULTECH 2023)*, pages 326-331
ISBN: 978-989-758-668-2; ISSN: 2184-2841

states will only converge asymptotically to the origin. Additionally, Linear SMC (LSMC) is concerned with low precision, decaying performance, and chattering issues that might overload the actuators. Using a nonlinear sliding manifold with continuous-based SMC methods is one approach to get around the chattering problem and slow convergence rate (F. Guo, 2019). Compared with LSMC, continuous-based SMC offers faster finite-time convergent response and accurate tracking (Yu, 1997). For instance, the work (O. Mechali L. X., 2022) deals with robust trajectory tracking of a quadrotor vehicle through a homogeneous terminal sliding mode control. Nonetheless, the controller in (O. Mechali L. X., 2022) is observer-based, resulting in more computational burden. Such a method does not fit our application, consisting of implementing the controller in Pixhawk 1 board. Furthermore, this autopilot is limited in terms of memory resources; thus, control performance might be compromised. To the best of the authors' knowledge, only a few research studies, such as (F. Guo, 2019) and (Falcón, Ríos, & Dzul, 2019), investigate a continuous SMC-based control for quadrotor aircraft designs with real-time implementation onboard a dedicated autopilot. The current effort's fundamental goal, inspired by (H. Rabiee, 2019), is to report experimental findings to bridge the gap between theoretical fronts and real-world situations.

The main scientific contributions of the current research can be summed up as follows:

- Inspired by the homogeneity theory, an IOHTC is proposed to deal with the fast dynamics' response of the attitude states. The proposed controller allows for mitigating the chattering of discontinuous SMC techniques compared to (S. Ullah, 2020) (Almakhles, 2020) (N. Wang, 2019) (Z. Hou, 2020).
- It is worth mentioning that the disturbance rejection does not require the design of an observer or an adaptation mechanism since the control law integrates a compensation term. Thus, resulting in alleviating the computational burden on the Pixhawk autopilot being memory-resource limited;
- terms of application, a beneficial model-based design methodology is used to incorporate the control algorithm inside the quadrotor autopilot. The suggested IOHTC method and three other controllers are compared in this study.

The following is the outline of this article. The preliminaries and the problem description are presented in Section 2. Then, in Section 3, the control method is presented along with a thorough mathematical analysis of the stability. The experimental results are critically discussed in Section 4. Finally, Section 5 concludes the paper and considers possible research directions.

2 PRELIMINARIES AND PROBLEM STATEMENT

2.1 Preliminaries

Lemma 1. (Xu, 2017). Consider the following system

$$\dot{x} = f(x), \quad x(0) = x_0, \quad x \in \mathbb{R}^n \tag{1}$$

If there exist C^1 Lyapunov function $V(x)\colon \mathrm{D} \to \mathbb{R}_+$ and some real constants $0 < c < \infty$ and $0 < \alpha < 1$, such that $\dot{V}(x) \leq -cV(x)^\alpha$; then, system (1) is finite-time stable for any given $x(t_0) \in \mathrm{D}_0 \subseteq \mathrm{D}$.

2.2 Problem Statement

The three differential equations governing the rotational dynamics of the quadcopter in the presence of external disturbances are given as in (F. Guo, 2019)

$$\begin{cases} \ddot{\Phi} = J_{xx}^{-1}[(J_{yy} - J_{zz})\dot{\theta}\dot{\psi} - c_\Phi \dot{\Phi}^2 - J_r\bar{\omega}\dot{\theta} + u_\Phi + d_\Phi^{\mathrm{ext}}], \\ \ddot{\theta} = J_{yy}^{-1}[(J_{zz} - J_{xx})\dot{\Phi}\dot{\psi} - c_\theta \dot{\theta}^2 + J_r\bar{\omega}\dot{\Phi} + u_\theta + d_\theta^{\mathrm{ext}}], \\ \ddot{\psi} = J_{zz}^{-1}\left[(J_{xx} - J_{yy})\dot{\Phi}\dot{\theta} - c_\psi \dot{\psi}^2 + u_\psi + d_\psi^{\mathrm{ext}}\right], \end{cases} \tag{2}$$

To elaborate an adequate control model of the quadrotor, state-space representation can be used to reformulate the mathematical model (equation 2) as

$$\begin{cases} \dot{\mathrm{x}}_1 = \mathrm{x}_2, \\ \dot{\mathrm{x}}_2 = J_{xx}^{-1}\left((J_{yy} - J_{zz})\mathrm{x}_4\mathrm{x}_6 + u_\Phi + d_\Phi^{\mathrm{lum}}\right), \\ \dot{\mathrm{x}}_3 = \mathrm{x}_4, \\ \dot{\mathrm{x}}_4 = J_{yy}^{-1}\left((J_{zz} - J_{xx})\mathrm{x}_2\mathrm{x}_6 + u_\theta + d_\theta^{\mathrm{lum}}\right), \\ \dot{\mathrm{x}}_5 = \mathrm{x}_6, \\ \dot{\mathrm{x}}_6 = J_{zz}^{-1}\left((J_{xx} - J_{yy})\mathrm{x}_2\mathrm{x}_4 + u_\psi + d_\psi^{\mathrm{lum}}\right), \end{cases} \tag{3}$$

Where $\mathrm{x} \triangleq \begin{bmatrix} \Phi & \dot{\Phi} & \theta & \dot{\theta} & \psi & \dot{\psi} \end{bmatrix} \in \mathbb{R}^{12}$ the state vector. the design of the control law follows from the perturbated second-order nonlinear system given below

$$\begin{cases} \dot{\chi}_1(t) = \chi_2(t), \\ \dot{\chi}_2(t) = f_\Theta(\chi_2, t) + g_\Theta(t)u_\Theta(t) + d_\Theta^{\mathrm{lum}}(d_\Theta^{\mathrm{ext}}, d_\Theta^{\mathrm{unm}}, t), \\ Y_1(t) = \chi_1(t). \end{cases} \tag{4}$$

Where $X_\Theta \triangleq [\chi_1 \quad \chi_2]^T \in \mathbb{R}^{3\times 2}$ is the vector of states, and $\chi_1 \triangleq \Theta = [\mathrm{x}_1 \quad \mathrm{x}_3 \quad \mathrm{x}_5]^T = [\Phi \quad \theta \quad \psi]^T$ $\chi_2 \triangleq \dot{\Theta} = [\dot{\Phi} \quad \dot{\theta} \quad \dot{\psi}]^T = [\mathrm{x}_2 \quad \mathrm{x}_4 \quad \mathrm{x}_6]^T$, and

$u_\Theta \triangleq [u_\Phi \quad u_\theta \quad u_\psi]^T \in \mathbb{R}^3$ is the vector of control inputs, $\mathcal{Y}_1 \triangleq [\Phi \quad \theta \quad \psi]^T \in \mathbb{R}^3$ is the vector of controlled outputs, and the uncertain function $d_\Theta^{\text{lum}} \triangleq \left[d_\Phi^{\text{lum}} \quad d_\theta^{\text{lum}} \quad d_\psi^{\text{lum}}\right]^T \in \mathbb{R}^3$ stands for the total lumped disturbances, i.e., unmodeled dynamics and external load perturbations. The functions $f_\Theta(\chi_2, t), g_\Theta(t)$ are defined as follow:

$$f_\Theta(\chi_2, t) \triangleq \begin{bmatrix} f_\Phi \\ f_\theta \\ f_\psi \end{bmatrix} = \begin{bmatrix} J_{xx}^{-1}(J_{yy} - J_{zz})\dot{\theta}\dot{\psi} \\ J_{yy}^{-1}(J_{zz} - J_{xx})\dot{\Phi}\dot{\psi} \\ J_{zz}^{-1}(J_{xx} - J_{yy})\dot{\Phi}\dot{\theta} \end{bmatrix} \tag{5}$$

$$g_\Theta(t) \triangleq [g_\Phi \quad g_\theta \quad g_\psi]^T = \left[J_{xx}^{-1} \quad J_{yy}^{-1} \quad J_{zz}^{-1}\right]^T \tag{6}$$

Definition 1. (Robust tracking control problem). The considered control problem of our study consists of designing robust finite-time SMC laws $\boldsymbol{u_\Theta} = [\boldsymbol{u_\Phi} \quad \boldsymbol{u_\theta} \quad \boldsymbol{u_\psi}]^{\boldsymbol{T}}$ for the attitude system affected by perturbations in (4), such that: ***(i)*** The attitude tracking errors tend to the origin in finite-time, i.e., for $\forall \boldsymbol{e_1^\Theta(t)} \triangleq \boldsymbol{\Theta(t) - \Theta_d(t)}$, There exist a constant $\boldsymbol{T_\Theta}$, such that: $\lim_{\boldsymbol{t \to T_\Theta}} \boldsymbol{e_1^\Theta(t) = 0}, \ \forall \boldsymbol{t > T_\Theta}$, where $\boldsymbol{\Theta_d}$ is the desired reference signal for the attitude system. ***(ii)*** The controller must ensure robustness against uncertainties and disturbances. ***(iii)*** The control signal is chattering-free.

3 CONTROL DESIGN AND STABILITY ANALYSIS

3.1 Control Design

Let the attitude-tracking error and its dynamics be defined as:

$$\begin{cases} e_1^\Theta(t) \triangleq \Theta(t) - \Theta_d(t) \\ e_2^\Theta(t) \triangleq \dot{\Theta}(t) - \dot{\Theta}_d(t) \end{cases} \tag{7}$$

$$\begin{cases} e_1^\Theta(t) = \left[e_1^\Phi \quad e_1^\theta \quad e_1^\psi\right]^T \in \mathbb{R}^3, \\ e_2^\Theta(t) = \left[e_2^\Phi, e_2^\theta, e_2^\psi\right]^T \in \mathbb{R}^3, \end{cases} \tag{8}$$

The derivatives of the above expressions are given as:

$$\begin{cases} \dot{e}_1^\Theta = e_2^\Theta, \\ \dot{e}_2^\Theta = \ddot{\Theta} - \ddot{\Theta}_d. \end{cases} \tag{9}$$

The Traditional Twisting Control (TTC) algorithm is given as:

$$\begin{cases} \bar{u}_\Theta = -k_{\Theta_1}\lceil e_1^\Theta \rfloor^{\frac{1}{3}} - k_{\Theta_2}\lceil e_2^\Theta \rfloor^{\frac{1}{2}} + \vartheta_\Theta, \\ \dot{\vartheta}_\Theta = -k_{\Theta_3}\lceil e_1^\Theta \rfloor^0 - k_{\Theta_4}\lceil e_2^\Theta \rfloor^0. \end{cases} \tag{10}$$

Remark 1. It has been shown in work (Falcón, Ríos, & Dzul, 2019) that the TTC controller generates a higher frequency, i.e., chattering in its control signal. Therefore, limiting its implementation in practice. Hence, to improve its performance, we propose to: ***(i)*** Design a smooth hyperbolic function to mitigate the chattering effect as $\mathcal{F}(e_1^\Theta) \triangleq (e_1^\Theta)^\varpi[\tanh(e_1^\Theta/\upsilon)]^\varpi$, where ϖ, υ are positive constants that are related to $\mathcal{F}$ function. ***(ii)*** Integrate the sliding function $s_\Theta = e_2^\Theta + k_s e_1^\Theta$ in the TTC's algorithm to enhance the robustness and tracking.

Consequently, by introducing the following control law for the attitude system

$$\begin{cases} \bar{u}_\Theta \triangleq -k_{\Theta_1}|e_1^\Theta|^{\frac{1}{3}}\mathcal{F}(e_1^\Theta) - k_{\Theta_2}|s_\Theta|^{\frac{1}{2}}\mathcal{F}(s_\Theta) + \vartheta_\Theta, \\ \dot{\vartheta}_\Theta \triangleq k_{\Theta_3}|e_1^\Theta|^0\mathcal{F}(e_1^\Theta) - k_{\Theta_4}|s_\Theta|^0\mathcal{F}(s_\Theta), \\ s_\Theta = e_2^\Theta + k_s e_1^\Theta. \end{cases} \tag{11}$$

The final attitude controller is formulated as:

$$u_\Theta \triangleq [g_\Theta]^{-1}\begin{bmatrix} -k_{\Theta_1}|e_1^\Theta|^{\frac{1}{3}}\mathcal{F}(e_1^\Theta) - \\ k_{\Theta_2}|s_\Theta|^{\frac{1}{2}}\mathcal{F}(s_\Theta) + \vartheta_\Theta - f_\Theta \end{bmatrix} \tag{12}$$

3.2 Stability Analysis of the Closed Loop System

Theorem 1. Consider the nonlinear perturbated attitude system (4) and the designed control law u_Θ given in (11). Then, the attitude tracking errors are globally finite-time stable at the origin.

Proof. Since the attitude dynamics are similar, we consider the stability proof of the roll angle. The closed-loop dynamics for the roll variable Φ can be described as:

$$\begin{cases} \dot{e}_1^\Phi = e_2^\Phi, \\ \dot{e}_2^\Phi = -k_{\Phi_1}|e_1^\Phi|^{\frac{1}{3}}\mathcal{F}(e_1^\Phi) - k_{\Phi_2}|s_\Phi|^{\frac{1}{2}}\mathcal{F}(s_\Phi) + \varsigma_\Phi, \\ \dot{\varsigma}_\Phi = -k_{\Phi_3}|e_1^\Phi|^0\mathcal{F}(e_1^\Phi) - k_{\Phi_4}|s_\Phi|^0\mathcal{F}(s_\Phi) - \Phi_d^{(3)}, \\ s_\Phi = e_2^\Theta + k_s e_1^\Theta. \end{cases} \tag{13}$$

Where $\varsigma_\Phi = \vartheta_\Phi - \ddot{\Phi}_d$. The third expression in (12) can be associated with differential inclusion (DI) $\dot{\varsigma}_\Phi \in -k_{\Phi_3}|e_1^\Phi|^0\mathcal{F}(e_1^\Phi) - k_{\Phi_4}|s_\Phi|^0\mathcal{F}(s_\Phi) + [-\lambda, \lambda]$ which is basically $\dot{\varsigma}_\Phi \in -k_{\Phi_3}|e_1^\Phi|^0\text{sign}(e_1^\Phi) - k_{\Phi_4}|s_\Phi|^0\text{sign}(s_\Phi) + [-\lambda, \lambda]$ .Therefore, it is associated with DI $\dot{x} \in \text{F}(x)$, where the set valued map F is given by $\text{F}(x) = \{y \in \mathbb{R}^n | y = [e_2^\Phi, \varsigma_\Phi, \rho]^T\}$, for all $\rho \in -k_{\Phi_3}|e_1^\Phi|^0\mathcal{F}(e_1^\Phi) - k_{\Phi_4}|s_\Phi|^0\mathcal{F}(s_\Phi) + [-\lambda, \lambda] \subset \mathbb{R}$. This DI is

homogeneous of degree $q_\Phi = -1$ with weights $r_\Phi = [3,2,1]^T$ (Falcón, Ríos, & Dzul, 2019).

Let the following candidate Lyapunov function be proposed for system (10)

$$\begin{aligned} V_\Phi(e_1^\Phi, e_2^\Phi, \varsigma_\Phi) = {} & \alpha_1|e_1^\Phi|^{\frac{5}{3}} + \alpha_2 e_1^\Phi s_\Phi + \alpha_3|s_\Phi|^{\frac{5}{2}} \\ & + \alpha_4 e_1^\Phi\left(|\varsigma_\Phi|^2\mathcal{F}(\varsigma_\Phi)\right) - \alpha_5 s_\Phi \varsigma_\Phi^3 \\ & + \alpha_6|\varsigma_\Phi|^5, \end{aligned} \quad (14)$$

Where $\alpha_j = [\alpha_1, \dots, \alpha_6]^T \in \mathbb{R}^6, j = \overline{1,6}$ is a coefficients vector. The time derivative of $V_\Phi(e_1^\Phi, e_2^\Phi, \varsigma_\Phi)$ is computed as:

$$\begin{aligned} \dot{V}_\Phi = \mathcal{M} = {} & \beta_1|e_1^\Phi|^{\frac{4}{3}} + \beta_2 e_\Phi \text{sign}^{\frac{1}{2}}(s_\Phi) - \beta_3 \text{sign}^{\frac{2}{3}}(e_1^\Phi)s_\Phi \\ & + \beta_4 \text{sign}^{\frac{1}{3}}(e_1^\Phi)\text{sign}^{\frac{3}{2}}(s_\Phi) + \beta_5|s_\Phi|^2 \\ & - \beta_6 e_1^\Phi \varsigma_\Phi + \beta_7|e_1^\Phi||\varsigma_\Phi| \\ & - \beta_8 e_1^\Phi \text{sign}^0(s_\Phi)|\varsigma_\Phi| \\ & - \beta_9 \text{sign}^{\frac{3}{2}}(s_\Phi)\varsigma_\Phi - \beta_{10} s_\Phi \text{sign}^2(\varsigma_\Phi) \\ & + \beta_{11}\text{sign}^0(e_1^\Phi)s_\Phi|\varsigma_\Phi|^2 \\ & - \beta_{12}|e_1^\Phi||\varsigma_\Phi|^2 - \beta_{13}\text{sign}^{\frac{1}{3}}(e_1^\Phi)\varsigma_\Phi^3 \\ & - \beta_{14}\text{sign}^{\frac{1}{2}}(s_\Phi)\varsigma_\Phi^3 + \beta_{15}|\varsigma_\Phi|^4 \\ & + \beta_{16}\text{sign}^0(e_1^\Phi)\text{sign}^4(\varsigma_\Phi) \\ & + \beta_{17}\text{sign}^0(e_2^\Phi)\text{sign}^4(\varsigma_\Phi). \end{aligned} \quad (15)$$

Where $\beta_1 = \alpha_2 k_{\Phi_1}, \beta_2 = \alpha_2 k_{\Phi_2}, \beta_3 = \frac{5}{3}\alpha_1, \beta_4 = \frac{5}{2}\alpha_3 k_{\Phi_1}, \beta_5 = \frac{5}{2}\alpha_3 k_{\Phi_2} - \alpha_2, \beta_6 = \alpha_2, \beta_7 = 2\alpha_4 k_{\Phi_3}, \beta_8 = 2\alpha_4 k_{\Phi_4}, \beta_9 = \frac{5}{2}\alpha_3, \beta_{10} = \alpha_4, \beta_{11} = 3\alpha_5 k_{\Phi_3}, \beta_{12} = 3\alpha_5 k_{\Phi_4}, \beta_{13} = \alpha_5 k_{\Phi_1}, \beta_{14} = \alpha_5 k_{\Phi_2}, \beta_{15} = \alpha_5, \beta_{16} = 5\alpha_6 k_{\Phi_3}, \beta_{17} = 5\alpha_6 k_{\Phi_4}$. The Lyapunov function V_Φ given in (13) is homogeneous of degree $m = 5$. Thus, there exist a continuous homogeneous function $\mathcal{M}$ of degree $m + q_\Phi = 4$ such that $\dot{V}_\Phi \leq -\mathcal{M}$. Hence, there exist a real $\gamma_\Phi > 0$ such that $\mathcal{M} \geq \gamma_\Phi V_\Phi^{\frac{4}{5}}$. Therefore, $\dot{V}_\Phi \leq -\gamma_\Phi V_\Phi^{\frac{4}{5}}$. This implies that the tracking errors are finite-time stable at the origin. Furthermore, since the control system is homogeneous, the stability property is global. The expression of the settling-time can be obtained by solving the differential equation $\dot{V}_\Phi \leq -\gamma_\Phi V_\Phi^{\frac{4}{5}}$. This can be achieved by appealing to the separation of variables method. Thus, by separating the variables and then integrating both sides of the equation, we get $\int_0^t \frac{1}{V_\Phi^{\frac{4}{5}}} dV_\Phi \leq \int_0^t -\gamma_\Phi dt$. Then the following expression is obtained $5V_\Phi^{\frac{1}{5}} \leq -\gamma_\Phi t$. Finally, we can get $T_\theta \leq \frac{5}{\gamma_\Phi} V_\Phi^{\frac{1}{5}}$. It follows from Lemma 1 that the tracking errors are finite-time stable. Thus, completing the proof.

4 EXPERIMENT RESULTS AND DISCUSSION

4.1 Control Gains Tuning

The gains of the controller are tuned by using the *"Optimization Toolbox"*. Two blocks are used to optimize the parameters: *(i)* Check Step Response Characteristics (CSRC) block; *(ii)* Check Against Reference (CAR) block. In the general case, these two optimization blocks are inserted in the output of the control loop, as shown in Fig. 1. The CSRC block checks that a signal satisfies the step response bounds during simulation (Settling-time, Rise-time, % Overshoot, and % Undershoot). CAR block checks that a signal remains within the tolerance bounds, at steady-state, of a reference signal during the simulation.

CSRC, CAR blocks ensure that a signal remains within specified time-domain characteristic bounds. In our case, these bounds are chosen for a unit step response, as shown in Table.

4.2 Tracking Experiment Under Load Disturbances

To quantify the superior performance achieved by the presented controller, comparative studies are conducted among the following controllers: PID controller, Back-Stepping Controller (BSC), Integral Back-Stepping Sliding Mode Controller (IBSSMC)

Table 1: Specified time-domain characteristic bounds for position states.

States	Optimization Block	Characteristics	Value
Φ, θ, ψ	CSRC	Settling-time (s)	≤ 2 s
		Rise-time (s)	≤ 4 s
		Overshoot (%)	≤ 30 %
		Undershoot (%)	≤ 5 %
	CAR	Amplitudes	$1 - \exp(-\text{linspace}(0,20)/2)$
		Absolute tolerance	$\text{eps}^{(1/3)}$
		Relative tolerance	0.01

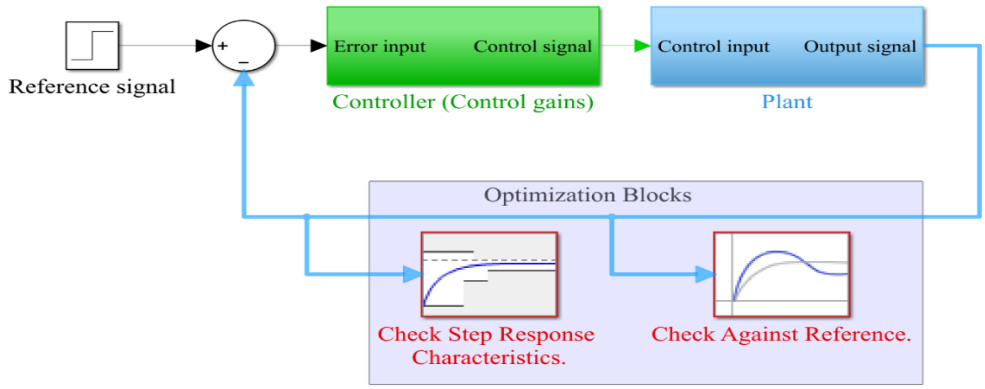

Figure 1: Integration of the optimization blocks in the closed-loop control system.

(Falcón, Ríos, & Dzul, 2019), and the proposed controller. A load perturbation of 130 grams is attached to the edge of the rear-left arm of the quadrotor. The attitude variables are commanded to track a time-varying reference trajectory given by: $\Phi_d = 10\sin(0.08t), \theta_d = -10\sin(0.08t), \psi_d = -7.5\cos(0.08t)$.

Fig. 2 shows the experimental setup for the real-time controllers implementation and validation. The tracking states are displayed in Figure 4, whereas Figure 3 shows the tracking errors. From these two figures, it can be observed that the proposed control strategy ensures a robust tracking of the reference trajectory. Figure 4 also presents the control signals for all controllers, where we can notice that the control inputs of the proposed controller have no noticeable control switching (chattering). Well-known performance indexes are used to characterize the comparison of the achieved results. These include the Integral of the Absolute value of the Derivative of the input u (IADU) and Integral of Square Error (ISE). This improvement is quantified by the Relative Percentage Difference (RPD) index as follows: ($u_\Phi \downarrow 60\%, u_\theta \downarrow 36.08\%, u_\psi \downarrow 76.60\%$) compared to IBSSMC.

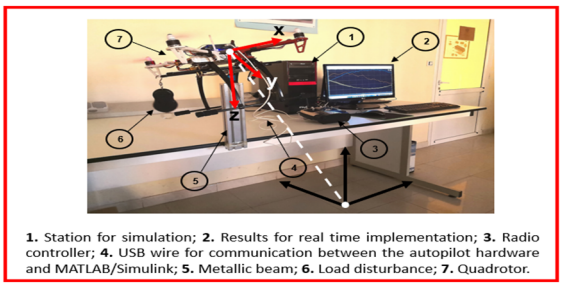

Figure 2: Experimental setup for real time control implementation.

5 CONCLUSION

This work proposed an IOHTC approach to design a robust attitude control law while considering lumped disturbances. The stability of the control system has been rigorously discussed based on a homogeneous-Lyapunov function. Results based on the real-time implementation in autopilot hardware are found to be consistent with the theoretical foundations. To thoroughly examine the capabilities of the synthesized controller, a comparative analysis based on various performance indices performed. Results witness the effectiveness and superiority of the proposed control law in terms of robustness, accuracy, and elimination of the chattering effect. Further studies will address Cartesian trajectory tracking with a real outdoor flight experiment.

REFERENCES

Almakhles, D. J. (2020). Robust Backstepping Sliding Mode Control for a Quadrotor Trajectory Tracking Application. IEEE Access, 5515-5525.

F. Guo, M. W. (2019). An Unmanned Aerial Vehicles Collaborative Searching and Tracking Scheme in Three-Dimension Space. IEEE 9th Annual International Conference on CYBER Technology in Automation, Control, and Intelligent Systems (CYBER) (pp. 1262-1266). Suzhou, China: IEEE.

Falcón, R., Ríos, H., & Dzul, A. (2019). Comparative analysis of continuous sliding-modes control strategies for quad-rotor robust tracking. Control Engineering Practice, 90, 241-256.

H. Rabiee, M. A. (2019). Continuous nonsingular terminal sliding mode control based on adaptive sliding mode disturbance observer for uncertain nonlinear systems. *Automatica*, 1-7.

Table 2: ISE and IADU performances indices for attitude control.

Controller	Index					
	IADU			ISE		
	Φ	θ	ψ	Φ	θ	ψ
PID	-	-	-	0.818	0.835	1.252
BSC	-	-	-	0.299	0.410	0.067
IBSSMC	1.125	1.383	1.111	0.103	0.068	0.006
PROPOSED	**0.449**	**0.884**	**0.260**	**0.024**	**0.014**	**0.005**

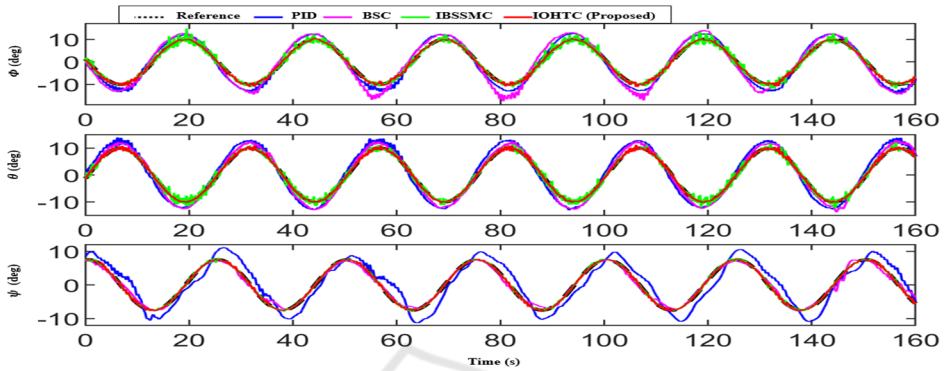

Figure 3: Plots of the Attitude states.

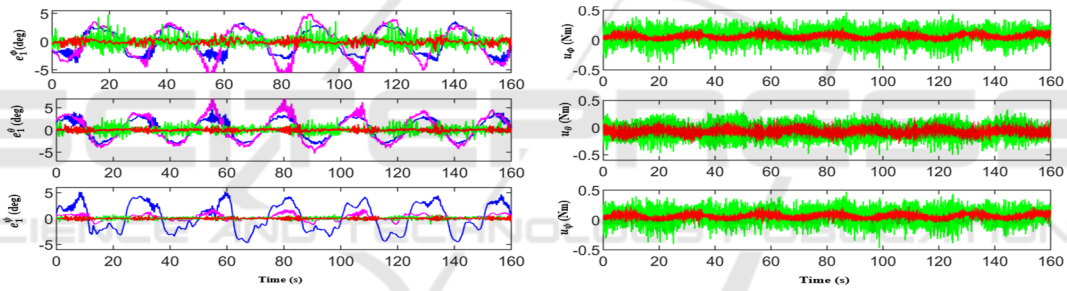

Figure 4: Plots of the tracking errors for the attitude states and the control signals.

N. Wang, Q. D. (2019). Hybrid finite-time trajectory tracking control of a quadrotor. *ISA Transactions*, 278-286.

O. Mechali, J. I. (2021). Distributed leader-follower formation control of quadrotors swarm subjected to disturbances. *IEEE International Conference on Mechatronics and Automation (ICMA)* (pp. 1442-1447). Japan: IEEE.

O. Mechali, J. I. (2021). Finite-Time Attitude Control of Uncertain Quadrotor Aircraft via Continuous Terminal Sliding-Mode-Based Active Anti-Disturbance Approach. *IEEE International Conference on Mechatronics and Automation (ICMA)* (pp. 1170-1175). Takamatsu, Japan: IEEE.

O. Mechali, L. X. (2022). Fixed-time nonlinear homogeneous sliding mode approach for robust tracking control of multirotor aircraft: Experimental validation. *Journal of the Franklin Institute*, 1971-2029.

S. Benmansour, D. F. (2023). Fuzzy Integral Sliding Mode Control of a Hyperdynamic Golf Swing Robot. *International Conference on Electrical Engineering and Control Applications.*

S. G. Khan, S. B. (2019). Experimental validation of an integral sliding mode-based LQG for the pitch control of a UAV-mimicking platform. *Advances in Electrical and Electronics Engineering*, 275-284.

S. Ullah, A. M. (2020). Robust integral sliding mode control design for stability enhancement of under-actuated quadcopter. *International Journal of Control, Automation and Systems*, 1671-1678.

Xu, Q. (2017). Continuous integral terminal third-order sliding mode motion control for piezoelectric nanopositioning system. *IEEE/ASME Transactions on Mechatronics*, 1828-1838.

Yu, M. Z. (1997). Terminal sliding mode control of MIMO linear systems. *IEEE Transactions on Circuits and Systems I: Fundamental Theory and Applications*, 1065-1070.

Z. Hou, P. L. (2020). Nonsingular terminal sliding mode control for a quadrotor UAV with a total rotor failure. *Aerospace Science and Technology*, 1-18.